Building and Environment 204 (2021) 108139

Contents lists available at ScienceDirect

Building and Environment

journal homepage: www.elsevier.com/locate/buildenv

Mitigating aerosol infection risk in school buildings: the role of natural ventilation, volume, occupancy and CO_2 monitoring

Alessandro Zivelonghi [a,b,*], Massimo Lai [c]

[a] Applied Mathematics, ITCS Lorgna-Pindemonte, Verona, Italy
[b] Power-Consulting Studio, San Pietro in Cariano, Verona, Italy
[c] Senior Research Scientist, Certara, UK

ARTICLE INFO

Keywords:
Airborne transmission
School classrooms
Natural ventilation
Covid-19
Gammaitoni-nucci
Riley-wells model
CO_2 monitoring

ABSTRACT

Issues linked to aerosol physics within school buildings and related infection risk still lack a proper recognition in school safety regulations. Limited spaces and limited available window-surfaces require to precisely investigate the seasonal airing factors and the occupancy/volume ratios in each classroom in order to assess the specific risk levels from viral loads of potentially infective sources. Moreover, most schools are still not provided with mechanical HVAC systems nor with air quality sensors. Fundamental questions are therefore: how the specific classroom volume and the specific airing cycle affects the long-range contagion risk in a given classroom? is linear social distancing the right way to assess a volumetric risk problem? We present here the results of an extended quantitative analysis based on the GN-Riley infection risk model applied to a real classroom scenario. The study discusses seasonality of the airing flow and the effectiveness of single and combined mitigation interventions, such as limiting student groups, equipping teachers with microphones, increasing classroom volumes, and equipping classrooms with CO_2 sensors to safely drive airing intervals. Moreover, we show experimental CO_2 concentrations as well as occupancy and airing factors monitored in real time in a real classroom scenario. In agreement with recent literature, the results emphasize the need for a dynamic evaluation of the complex risk function over the whole exposure time (and not just the monitoring of the istanteneous CO_2 concentration) in order to correctly control the infection risk from aerosolization.

1. Introduction

School classrooms are enclosed settings where students and teachers spend prolonged periods of time and therefore risky environments for airborne transmission of SARS-CoV2.

Airborne infections originate from viral aerosol formation and the cumulative nature of air saturation. As stated by Morawska et al. in Ref. [1] and recently recognized by WHO, "inhaling small airborne droplets is a probable third route of infection" in addition to transmission via larger respiratory droplets and direct contact with infected people or contaminated surfaces. Evidence of airborne transmission causing outbreaks in different enclosed environments was reported from the early stage of Covid-19 pandemics [2]. Outbreaks in schools have also been reported in different countries from the beginning of pandemics [3–5,6], albeit the definition of outbreaks may vary. In a study on Israeli schools based on extended slub-testing, however, the occurrence of airborne transmission as probable main cause of infection in crowded classes has been well documented [7].

In a school classroom, groups of students, usually between twenty and thirty individuals, share the same premises for hours with potentially insufficient ventilation. This increases the likelihood of coming into contact with virus-loaded aerosol droplets generated by one infective source (student or teacher). This issue is of concern also when social distancing is correctly implemented because of the volumetric and cumulative nature of aerosol clouds (Fig. 1). The hypothetical scenario of an infective asymptomatic source entering a school classroom should be carefully investigated for the potentially large consequences it carries and to define a comprehensive risk mitigation strategy. This approach is valid even if preventive countermeasures are applied to reduce the entrance probability of infective sources. In fact, this probability cannot be curbed to zero, particularly in densely populated areas, where higher density has been shown to correlate to an increase in epidemic curves [8]. As a further evidence, many school outbreaks were recently reported in regions where preventive quarantine was in force after school

* Corresponding author. Department of Applied Mathematics, ITCS Lorgna-Pindemonte, Verona, Italy.
E-mail address: ing.zivelonghi@gmail.com (A. Zivelonghi).

https://doi.org/10.1016/j.buildenv.2021.108139
Received 8 May 2021; Received in revised form 9 July 2021; Accepted 9 July 2021
Available online 15 July 2021

reopening, like e.g. in Veneto Region, Italy at the end of April 2021 [6].

Indirect oral transmission of SARS-CoV2 is believed to be effectively reduced through the frequent manual airing or by automated mechanical HVAC systems [9,10]. Proper ventilation has already been proven to significantly lower oral transmission of other diseases like tuberculosis and influenza in confined environments (e.g. Refs. [9,11,12]). Very recent (although still unpublished) measurements of SARS-CoV2 air concentrations in ventilated and non-ventilated hospital rooms performed by the Italian Regional Environmental Agency "ARPA Piemonte" further confirm this believe for the covid-19 case [13]. Besides natural ventilation, mechanical ventilation systems, when adequately configured, could be equally or even more effective in mitigating the aerosol diffusion [9]. Unfortunately, unlike hospitals, the majority of schools worldwide are not equipped with such systems and will not be, at least for the foreseeable future (including the coming 2021/2022 school year). The present study focused on natural (manual) ventilation in schools combined with other mitigation factors, but the model within certain approximations could account for ventilation levels controlled by HVAC systems too.

A comprehensive mitigation strategy for controlling the aerosol infection risk is presented here following a preliminary study in October 2020 by the main author [14]. The revised strategy includes now the critical effect of splitting large class groups in critically small classrooms, the impact of voice reduction with microphones as well as a control strategy via CO_2 sensors.

In the present work we separately investigated both infective sources (infective student and infective teacher) as well as cold- and hot-season conditions on the window airflow. We introduced into the GN model the indoor/outdoor thermal gradient to model the through-windows airflow during the cold season. Moreover, an illustrative CO_2 decay measure taken in a real classroom context in June 2021 is also presented, which has been used for the estimation of the effective airing factors in summer and for real time risk assessment. In appendix, the concept of cumulative risk is mathematically discussed for the specific circumstances of applying a GN-Riley approach with a cycled occupancy function.

2. Methods

2.1. Gammaitoni-Nucci model with thermal gradient airflow

The infection risk model used in the present analysis implements the well-known Wells-Riley like approach [15] extended in the Gammaitoni-Nucci (GN) model [16], which considers time evolution of the viral charge. The GN as well as more recent models are all based on the Wells-Riley assumption, i.e. that a "quantum" of viral charge, once inhaled, is infecting 63.2% of homogeneously exposed hosts by definition. They are also based on the assumption that newly produced viral particles are instantly diluted over the whole ambient volume (perfect-mixing) and that the emission rate parameter ER_q (i.e. the number of infective "quanta" generated per hour by each infective subject) is known, at least as an averaged $\overline{ER_q}$ value over the exposure time. Past models based on Wells-Riley, although simplistic, have been proven sufficiently accurate to account for infections caused by measles, tubercolosi and influenza in confined and ventilated environments. A recent paper, authored by several experts in the field [1], elucidated how a possible mechanism for transmission of SARS-CoV2 in confined spaces would be the formation of "light" aerosol droplets (i.e. < 5 μm in diameter, unlike "heavy" droplets, over 5 μm) that diffuse in the environment after being produced by an infected person. In the GN model, if the number of infective sources remains constant, the probability of infection for each subject at a given time t will only depend on the total concentration of viral particles supposed isotropically distributed in the volume V. This probability follows a well-known exponential law for increasing exposure time t, which strictly depends on the parameter $\overline{ER_q}$ and the ventilation ratio p/AER, where p is the average inhalation flow (related to pulmonary capacity) and AER is the inflow of clean air provided by natural or mechanical ventilation. To account for the complex phenomenon of viral inactivation and gravitational deposition on surfaces [17], the air exchange rate (AER) in (2–4) is more properly substituted from an *infective virus removal rate* ($IVRR = AER + \lambda + k$) which adds to the AER a viral inactivation factor (λ) and a particle deposition factor (k). For the purpose of this demonstration the small contribution of particle deposition on surfaces has been neglected based

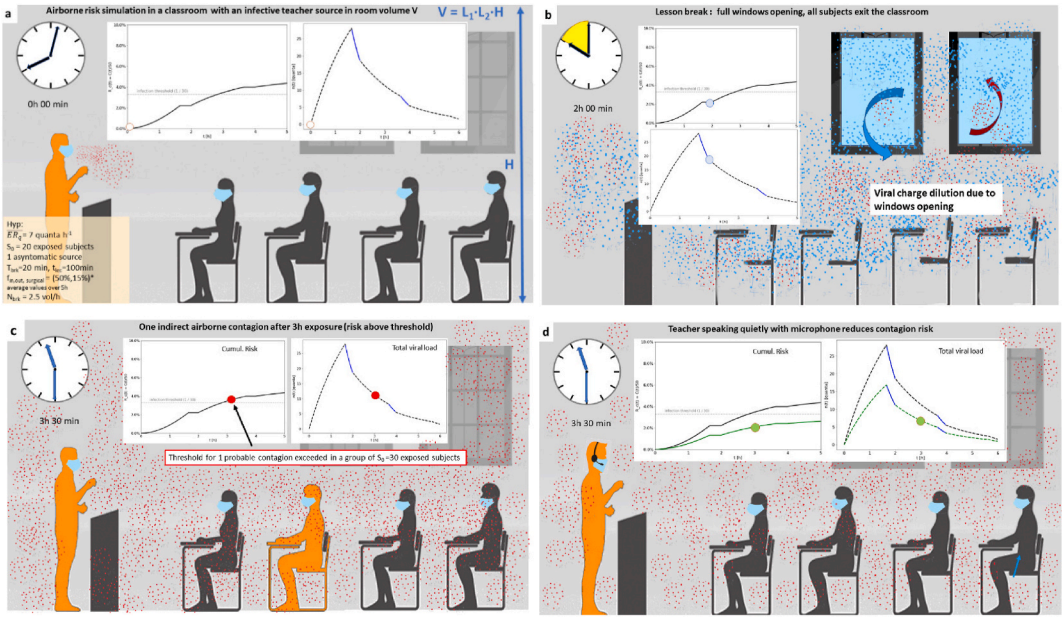

Fig. 1. Evolution of cumulative collective risk and total viral load in a classroom of volume V with a positive teacher source (long breaks of 20 min after lectures of 100 min). All presents are supposed to wear face masks with 80% effective filter efficiency. **a)** Situation at the beginning of the lesson, white markers indicate R (0) and n (0). **b)** Air change/dilution due to windows opening after the first break. **c)** Situation after 3 h with one probable infection. **d)** the same as in c) with less intense voicing preventing the contagion (teacher speaking through an amplified microphone).

on the fact that in winter heating systems in a classroom would tend to move air upward and in summer longer and almost continuous airing intervals can ensure a high level of ventilation. In addition, k values for standard non-heated environments are found in literature to be about 0.25 vol/h [18].

According to the GN model and following the nomenclature proposed by Buonanno [19], the risk of infection in a volume V, where one infective subject is present and the initial number of viral particles is n_0, has an analytical solution which can be expressed by the formula:

$$R_{airborne}(t) = 1 - e^{-\int_0^T IR^* n(t)dt} = 1 - e^{\left[-\frac{p\,\overline{ER_q}}{V}\,\frac{IVRR\cdot t + e^{-IVRR\cdot t} - 1 - \left(\frac{IVRR\cdot n_0}{\overline{ER_q}}\right)e^{-Nt} + \left(\frac{IVRR\cdot n_0}{\overline{ER_q}}\right)}{IVRR^2}\right]} = 1 - e^{\left[-\frac{p\,\overline{ER_q}}{V}\;\phi\left(t,\; n_0,\; \overline{ER_q},\; \overline{AER}\right)\right]} \quad (3)$$

In (3) the function ϕ(t) is also a function of source and ambient parameters, in particular of n_0, $\overline{ER_q}$, $\overline{AER}$:

$$\phi\left(t, n_0, \overline{ER_q}, \overline{AER}\right) = IVRR\left(\overline{AER}\right)\cdot t + e^{-IVRR\left(\overline{AER}\right)\cdot t} - 1 - \left(\frac{IVRR(AER)\cdot n_0}{\overline{ER_q}}\right)e^{-IVRRt} + \left(\frac{IVRR(AER)\cdot n_0}{\overline{ER_q}}\right) \quad (4)$$

The total viral load n(t) in the environment volume (measured in viral quanta), is given by an exponential saturation/decay law:

$$n(t) = \frac{\overline{ER_q}}{IVRR} + \left[n_0 - \frac{\overline{ER_q}}{IVRR}\right]e^{-IVRRt} \quad (5)$$

Throughout a full school day, the AER function should be also a general function of time but here for simplicity was assumed as a step-function, constant within lesson and break intervals with two different time-averaged values, respectively. A low $\overline{AER}_{background}$ value during all lessons (due to air leckages and a transom window supposed always open to ensure a minimum air exchange) and a higher $\overline{AER}_{break}$ value during breaks. However, different forms of the airing-function for manual airing during the hot and the cold season were introduced with different AER values (see Table 1). The resulting step function of AER(t) simulated a scheduled airing plan. In the present model we consider only natural ventilation (manual windows opening in a classroom), but with seasonal difference for the exchange rate intensity and duration due to manual airing ($AER^{winter} \neq AER^{summer}$; $t^{winter}_{man.\ airing} \neq t^{summer}_{man.airing}$) . Several factors influence natural ventilation in winter in a given classroom, the most important one beeing the temperature difference between the classroom and the outdoor space during windows opening. Other factors are wind direction and average wind speed, as well as geometric factors such as window size and position [17]. As for thermal effects, a high temperature difference $|T_i - T_e|$ between indoor and outdoor temperatures is expected during the cold season. Typically, the indoor temperature is maintained at $T_i = +20°C$ by the school heating system and an outdoor temperature of nearly 0 °C is usually taken as reference, so that $|T_i - T_e| = 20$ °C. This impact the through-window natural ventilation flow (considered here as an average over the exposure-time value). According to the recently revised Euronorm 16798–7:2018 [20] the single-sided airflow Q_w through an open windows with a given T-difference, is approximately estimated by the formula (valid for moderate wind velocities): $Q_w = 1800\cdot\frac{\rho_{a;ref}}{\rho_z}\cdot A_w(0.0035\cdot h_w\cdot|T_i - T_e|)^{0.5}$ with A_w, h_w, $\frac{\rho_{a;ref}}{\rho_z}$ beeing the total open windows area, the windows height and the air density ratio between reference air density and density of the considered zone. This implies an AER through windows opening which becomes function of the internal-external temperature difference:

Table 1
Model parameters and related value ranges. In brackets the controllable parameters.

Parameters	Description	Units	Range or value
t	*exposure time*	*h*	*0–5*
t_{brk}	*breaks duration*	*min*	*[5–30]*
t_{lec}	*lecture duration*	*min*	*[30−100]*
I	*number of infective sources*	*persons*	*1 in all simulations*
$S(t) = N(t) - I(t) + 1$	*number of susceptibles at time t*	*persons*	*15–30*
S_0	*number of susceptibles at time 0*		
N	*number of students per classroom*	*persons*	*15,20,30*
$C(t)$	*number of infected persons at time t*	*persons*	*0–30*
$R(t) = C(t)/S_0$	*infection risk*	-	*0-100%*
$ER_q(t)$	*Instantaneous emission rate by infective source*	*quanta* h^{-1}	*[5–25]*
$\overline{ER_q}$	*Time average emission rate (over exposure time)*		
$\bar{p}$	*average inhalation flow*	m^3h^{-1}	*0.6*
V	*classroom volume*	m^3	*170*
V_{eff}	*effective classroom volume*	m^3	*150*
$Q(t)$	*clean air inflow*	m^3h^{-1}	*85–1700*
$AER^{winter*}$	*Full open windows*	h^{-1}	*9.5*
	only transom windows open	h^{-1}	*2.5*
	**from EN16798–7:2018 @ΔT = 20°C*		
$AER^{summer**}$	*Full open windows + open door*	h^{-1}	*4.1–5.2*
	transom windows open + open door	h^{-1}	*2.5–3.8*
	***experimentally measured @ΔT = 0°C, V = 150m^3*		
λ	*viral inactivation factor*	h^{-1}	*0.5* [21]
k	*particle deposition factor*	h^{-1}	*0-0.25* [18]
$IVRR(t)$	*infective virus removal rate*	h^{-1}	*0–2.5*
$n(t)$	*viral quanta in ambient at time t*	*quanta*	*0–50*
n_0	*viral quanta at t = 0*	*quanta*	*≥0*
f_{in}	*mask reduction of inward viral load (susceptible person)*	-	*[15–30%] surgical [92%] FFP2*
f_{out}	*mask reduction of outward viral load (source)*	-	*[45–90%] surgical [94%] FFP2*

$$AER^{winter}_{windows} = \frac{1800}{V}\cdot\frac{\rho_{a;ref}}{\rho_z(T_i)}\cdot A_w(0.0035\cdot h_w\cdot|T_i - T_e|)^{0.5} \quad (6)$$

All curves were calculated for a typical classroom of volume 8 × 7 * 3 ≅ 170 m^3, with an effective volume for aerosol diffusion of 150 m^3. Hence, for such a standard classroom the resulting AER during windows opening results as:

$$AER^{winter}_{V=150} \cong 1675\, A_w(0.07\cdot h_w)^{0.5} \quad (7)$$

Fig. 2 indicates the temperature dependence of $AER_{V=150}$ assuming two typical values of (A_w, h_w) in a high-school classroom where windows are partially open. It is noted that geometrical windows parameters may also change strongly in different school buildings, or even in different classrooms in the same building. Investigating specific cases, however, lies outside the scope of the present work.

Windows opening implies a periodic activation of air exchanges per hour. Usually, they occur mainly during lesson breaks. In this case the IVRR function become also a periodic rectangular wave function over the full lesson time, with peaks influenced by higher values of the air exchange rate (AER) as due to partial windows opening (2 vol/h) or almost complete windows opening (up to 10 vol/h with high thermal gradient in winter as estimated according to EN 16798–7 [20] and up to 5 vol/h in summer (as measured experimentally). Another factor to be considered is the effective volume to be considered to dilute the aerosol viral cloud under the perfect mixing approximation. According to recent CFD simulations of aerosol cloud in classrooms [22], aerosol particles from a student source would not be diluted over the entire volume even

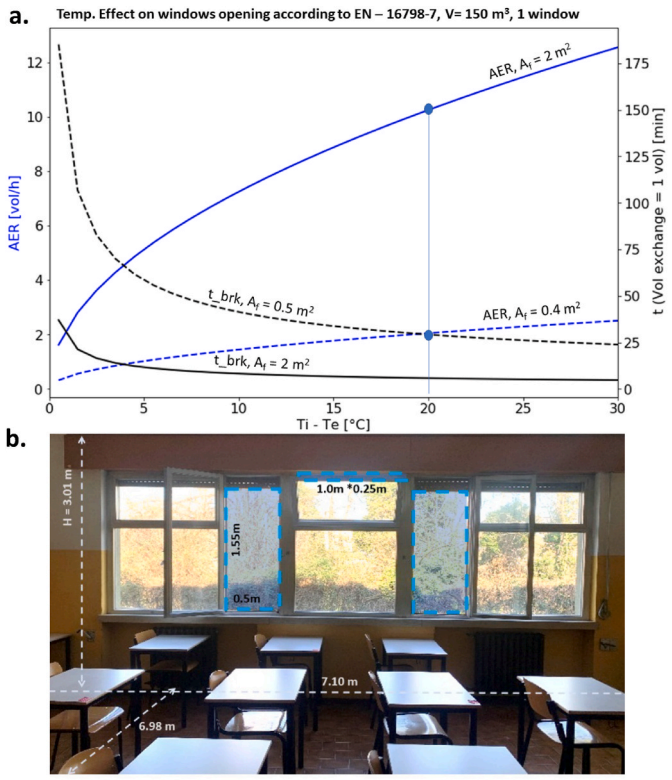

Fig. 2. **a**. Effect of indoor/outdoor temperature difference in winter on the air-exchange-rate by windows opening (blue curves) in a typical classroom according to the EN 16798–7 (single-sided ventilation) [20]. Marked blue dots indicate AER values used in simulations at Ti − Te = 20 °C. Duration of breaks to achieve AER = 1 h^{-1} volume are also shown. **b**. Effective area of openable windows (A_w) in a typical high school classroom of 150 m^3.

after a transient of 300s and the viral cloud volume during the first part of the emiss ion transient would be negligible compared to V. For these reasons an effective lower volume $V_{eff} = 0.85$ V in equations (3) and (11) was considered for the present analysis.

2.2. Air exchange rates from CO_2 decay

Besides providing theoretical values of AER^{winter} as driven mainly by thermal gradient, we preferred experimental estimations of the AER^{summer} since predictions from equation (6) would in fact lead to unrealistic zero airflow (nearly zero outdoor/indoor thermal gradient in summer in ventilated school buildings). In order to estimate the airing factors in a classroom from a CO_2 decay, one needs at least two conditions to be satisfied: 1. a starting point for the CO_2 concentration sufficiently distant from background before starting the decay (from previous occupancy of a certain number of people or through a dry ice probe as suggested by Allan & co-workers in [23]) and 2. no emission sources i.e. ERq = 0 during the decay, i.e. from the starting point until (ideally) the end of the decay (although an estimation with emission sources inside room is theoretically possible but it would introduce additional uncertainty and complication due to required estimation of the average CO_2 emission rate ER_{CO2}). The simplified procedure suggested by Allan is based on the identification of only two points of the exponential decay -and has the advantage to be simple and flexible (it works theoretically with any two points of the decay, provided a suitable time-distance is guaranteed). However, accuracy of the two-points method may be limited due to fluctuations of the CO_2 signal (which is evident from the experimental curve reported in Fig. 3a) probably linked to the 3D nature of the airflow (so that a 3D sensor network in classroom would be the ideal setup for very accurate measurements). Even with a single detector point, however, the estimation of the average airing factor could be more precise through a multi-point regression fit approach, aiming at the identification of the exponential decay function $C_{CO_2}(t)$:

$$C_{CO_2}(t) = C_0 + (C_{\text{start}} - C_0)e^{-\overline{AER}\cdot(t\ -\ t_{start})} \tag{9}$$

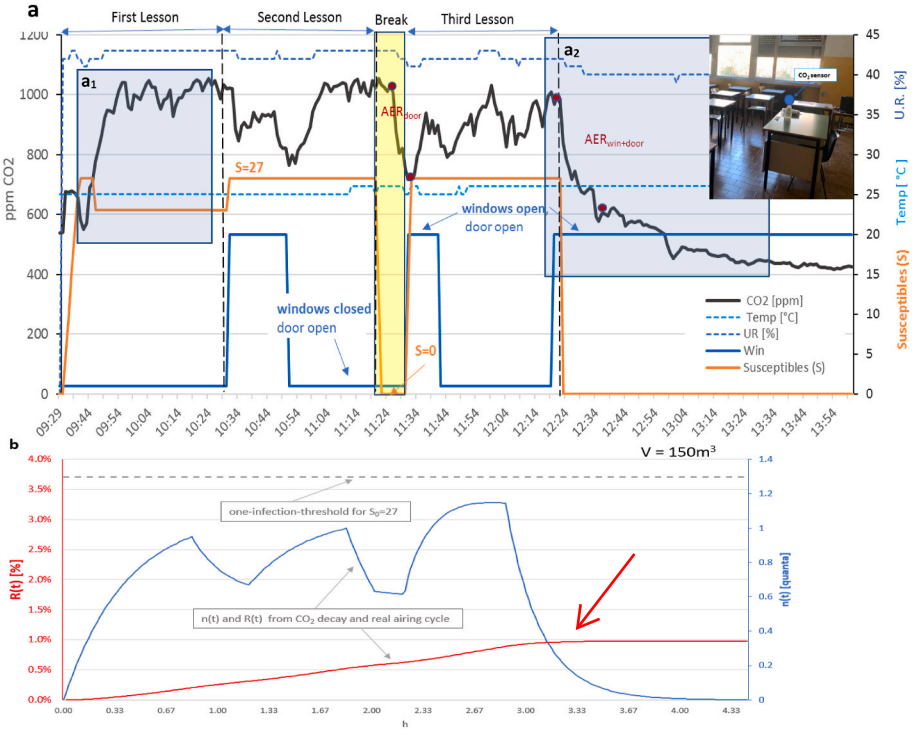

Fig. 3. a) CO_2 concentration (black solid line), manual airing scheme (blue solid line), number of susceptibles S (orange line), ambient temperature and RU, monitored in real time in an Italian high-school classroom during a school day in June 2021 with an MCH3 detector with dual NDIR sensor and sampling resolution of 1 min (detector position is also shown on the top-right). The light-blue regions indicate the parts of the CO_2 curve used for in-situ estimations: (**a_1**) fitting of the total viral emission rate $\overline{ER}_{q\,viral}$ and (**a_2**) fitting of $AER_{CR,OW}$, the airing factor during windows-opening for that classroom. **b)** Infection risk function calculated from equation 3 (red curve safely below the one-infection-threshold) and viral quanta evolution in ambient (blue curve) as estimated from input data in a) and equation 5.

from which an average $\overline{AER}$ could be derived using a "suitable" number of measured data-points. In (8), C_{start} is the initial CO_2 peak concentration reached just after all occupants left the classroom and the airing factors of interest have been activated (windows, door, etc). C_0 is the measured background (outdoor) CO_2 level. One may use equation (9) to account for the contribution of single or multiple (coupled) ventilation factors since the CO_2 decay depends on all ventilation factors acting in a given time interval. It is also noted that such indirect estimations already contain the effect of background ventilation due to room leakages and unperfect airtightness of the building.

In our experimental campaign, we aimed at measuring the combined effect of fully open side windows and fully open entrance door in a typical classroom. CO_2 concentrations were obtained with a calibrated portable dual NDIR detector placed in a high school classroom in North of Italy at the beginning of June (volume:149,8 m^3, maximum openable window area: 1.70 m^2 plus 0.25 m^2 central transom window) Three CO_2 curves were obtained in three different days (02–04.06.2021). One of these measurements is reported in Fig. 3, together with RU, T and occupancy curves. Although the entire school day was recorded, the useful time-windows for AER values fitting were during breaks (yellow region) and just after lessons' end (blue region), when all occupants left classroom (being instructed to leave both side windows and door open under surveillance of one author). The resulting values of $AER_{win+door}$ from backfitting, however, were strongly sensitive to the number of considered data points. In supplementary Fig.S1 the fitted airing factor was equal to 3.88 h-1 taking all data points, whereas considering only the first part of the decay (12 data points) a +40% higher value was obtained (5.40 h^{-1}). For comparison, values of 3.7–5.2 h^{-1} were attained with the two-points method depending on the distance of the second point from the starting point. Notably, the experimental AER values were in-line with target value of 5 air exchanges per hour recommended by the Harvard Healthy Buildings program [23].

A slight but visible change in the exponential decay is indeed observable not only in these decay curves but also in those reported in Ref. [23], a phenomenon the authors cannot explain so far.

As said, these AER estimations are representative for the summer season only and are affected by several uncertainties. Above all, probe positioning and distance of the sensor from individuals moving nearby. In particular, we observed a sudden decrease of CO_2 concentration at around 12 a.m. on the measure taken on June 03, 2021 (clearly visible in Fig. 3a) as due to local air movement caused by a teacher staying close to the detector for at least 12 min during lesson. Other minor uncertainty factors were detector accuracy (±40 ppm @22 °C by detector manufacturer), resolution (1 ppm), temperature and R.U. variation upon average (26 °C ± 1 °C and 41% ± 4% respectively).

2.3. Face masks modelling

To account for the effect of PPE (personal protective equipment, in this case, face masks) in reducing both the number of viral particles generated by infective subjects, and also reducing the likelihood of inhalation of viral particles by exposed subjects, we introduced two scaling factors:

(1- f_{out}), which represents the fractional reduction of the generated viral load, and
(1- f_{in}), which represents the fractional reduction of inhaled viral load,

Under the assumption that all subjects are wearing a mask. Eq. (3) can then be rewritten as:

$$R^{mask}(t) = 1 - e^{\left[-(1-f_{out})(1-f_{in})\ \frac{p\ \overline{ER_q}}{V}\ \phi\left(t,\ n_0,\ \overline{ER_q},\ AER\right)\right]} \tag{10}$$

If masks are not being worn, f_{in} and f_{out} are both zero. The extent of efficacy of face masks in reducing airborne transmission is the subject of still ongoing debate, although a general wide agreement on their importance as mitigation factor has been accepted. Some recent results [11] strongly supported the effectiveness of face masks in reducing the spread of infected aerosol droplets during exhalation, under the condition that the mask is correctly and permanently worn by both the infected and the susceptible subjects. The estimated efficacy of surgical masks in filtering the airborne viral load upon inhalation, represented by f_{in}, varies in the available literature. Some authors (e.g. Ref. [24]) estimate the value to be close to zero, claiming that masks can only filter "large" droplets (>5 μm), but more recent measurements suggest that surgical masks may actually be able to filter even "small", i.e. sub-micrometric, droplets [25]. In the present analysis, we considered a possible range of values 0–0.3 for fin which is in line for surgical masks. As for the efficacy in filtering the exhaled viral load, the parameter f could have a value as high as 0.95 [11] in the case of a perfectly adhering surgical mask worn the whole time. In a classroom environment, however, it will be difficult to ensure complete and continuous compliance over the many hours of a typical school day. For instance, a recommendation by the italian local scientific committees as of October 2020, is to wear masks for as long as possible, but to allow their occasional removal as long as social distancing is respected. Since mask filtering effectiveness varies from person to person and over the total exposure time, a rather large variation interval (from 50% to 100%) was considered for the filtering effectiveness.

2.4. Zero-infection condition

For at least one infection to occur, the cumulative risk $R_{cum}(t) = C(t)/S_0$ must be greater than $1/S_0$. Therefore, the condition for zero infections to occur over the total exposure time (5h) is:

$$R_{cum}(t=5h) = R_{5h} < \frac{1}{S_0} \quad \Leftrightarrow \quad R_0^{airborne} < 1 \tag{11}$$

and not $R_{lec,i}$ (t) < $1/S_0$. It is noted that in a classroom with one infective source the condition (13) corresponds to keeping the basic reproduction number $R_0^{airborne}$ below one, since, by definition $R_0^{airborne}$ = C/I=C and C = $R_{5h}S_0$. It is finally remarked that a conservative safety approach should aim at keeping the reproduction number below one at the end of each school day, even in case of an infective source entered a classroom.

2.5. Average emission rate for SARS-CoV2

A correct estimation for the emission rate parameter ER_q is the most critical assessment in the GN-Riley approach. Firstly, this parameter varies over the exposure time so that one should better speak of an instantaneous $ER_q(t)$ and a time averaged $\overline{ER}_q$. Secondly, at a certain time point, $ER_q(t)$ could theoretically be computed from the size distribution of the emitted aerosol droplets at that particular time, by integrating over the emitted particle size up to a cut-off size value of 10 μm:

$$ER_q(t) = p(t) \cdot c_{RNA} \cdot c_i \int_0^{10\mu m} N_d(D,t) dV_d(D) \tag{12}$$

Microdroplets populations in the emitted aerosol vary depending on the specific voice activity (voiced counting, whispered counting, unmodulated vocalization, breathing). First a short note on the chosen cut-off value. It is now generally accepted that particles up to 100 μm can travel long distances in air and should also be considered aerosol particles [26,27]. This fact however, does not imply that such particles should be considered in the present study, since they are in fact generated in specific events like sneezing and coughing and not in the "every-day" average situation the present model is trying to represent. Secondly, because of the filtering effects of face masks supposed worn by

all students and teachers in the present model (section 2.4), the emitted particle distribution would not contain such large size aerosol droplets. Finally, even during a cough event, it has been well documented that such large size particles are an irrelevant percentage for aerosolization as stated in Ref. [28] *"droplets of less than one-micron size represent 97% of the total number of measured droplets contained in the cough aerosol"*).

As proposed by Morawska [29], the emission rate of one specific expiratory activity can be well approximated with a 4-channel particle size distribution where the time dependent droplet distribution $N_d(D,t)$ is assumed constant during that specific activity (becoming $N_d^j(D)$). A time-independent average $\overline{ER}_q^j$ for that emission activity j can then be computed as:

$$\overline{ER}_q^j = \frac{1}{t_j}\int_0^{t_j} ER_q^j(t)dt \approx c_{RNA}\cdot c_i \cdot \overline{p}^j \cdot \sum_{i=1}^{4} \overline{N}_{D,i}^j \cdot \overline{V}_{D,i}^j \tag{13}$$

In (14) the parameter c_v is the viral load in the sputum (viral RNA copies mL^{-1}) to be estimated experimentally via clinical assessments of viral loads, c_i is a conversion factor having units in quanta•RNA copies^{-1} (ratio between one infective quantum and the infective dose), $\overline{p}^j$ is the average pulmonary inhalation rate ($m^3\ h^{-1}$) related to a particular j-th body-activity (resting, standing, walking, etc). $\overline{N}_{D,i}^j \cdot \overline{V}_{D,i}^j$ is the product between the average droplet density and the average droplet volume ($mL\ m^{-3}$) in one of the 4 channels of a typical droplet distribution expelled during voicing or breathing. For SARS-type viruses, experimental estimations of all parameters in equation (13) are reported in Refs. [19,30,31].

In addition, while modelling the real behaviour of a teacher or a student during the whole exposure time, one should consider a further time-average of (13). The reason is that both potential sources (during teaching or while attending lesson) do not behave permanently in one fixed category of vocal activity and pulmonary rate over the emission time. Therefore, the overall effective emission rate $\overline{ER}_q$ to be used in the differential GN model is in fact a double average integral (once over the size distribution and once over the emission time):

$$\overline{ER}_q = \frac{1}{t}\int_0^t ER_q(t)dt = c_{RNA}c_i\frac{1}{t}\int_0^t p(t)\left[\int_0^{10\mu m} N_d(D,t)dV_d(D)\right]dt \tag{14}$$

One way to estimate $\overline{ER}_q$ is to consider a student as a resting person and a teacher as a standing person, both involving *three* distinct major activities relevant for the emission process (breathing, speaking loud and speaking quietly) with weights depending on the specific "average" situation. Based on this rationale, equation (14) could be approximated as:

$$\overline{ER}_q \approx \frac{1}{t}\sum_{j=1}^{3} t_j \overline{ER}_q^j = \tag{15}$$

$$= \frac{1}{t}\left(t_{breath}\overline{ER}_q^{breath} + t_{sp.loud}\overline{ER}_q^{speak.loud} + t_{sp.quiet}\overline{ER}_q^{speak.quiet}\right)$$

Calculation details of the $\overline{ER}_q$ for the infective student and infective teacher cased used in all simulations are reported in appendix (Table A1). An alternative but more complex approach (which was not considered here) is that of introducing a normal probability distribution of ERq values instead of average constant values over the exposure time [32]. In our model, we derived values of $\overline{ER}_q^j$ for specific emission activities from Buonanno et al. [19] and estimated $\overline{ER}_q$ based on the approximation of equation (15) for both cases (student and teacher). Three "voice activity" levels and their related effective times t_j were considered (breathing without speaking, breathing during quietly speaking and loudly speaking). In fact, during teaching one may observe speaking periods of the teacher alternated with pauses and variation of the voice volume (which may vary considerably during lesson [33]). The same for students who may put questions or comments and randomly vary their voice activity and intensity. Although a precise estimation of such parameters would require a dedicated measurement campaign and may vary from different subjects, average values were selected from reported ranges in literature and justified assumptions on the different activity times are provided. Teachers spend usually one or 2 h only in a given classroom, and they are speaking most of this time. In primary and secondary schools, however, they may also speak loudly and sometimes screaming. This causes higher average values of $\overline{ER}_q^{teacher}$ and makes teachers a potentially greater viral source compared to students. In the present analysis, the estimated value was about 32 quanta h^{-1} for an infective teacher speaking at a moderately high volume, whereas a half value of 16 quanta h^{-1} was supposed for the same subject speaking quietly through a microphone. For infective students sitting at their desk most of the time while attending lessons, lower values of $\overline{ER}_q^{stud}$ were estimated, as they were considered resting persons speaking less frequently than teachers.

2.6. Determination of infection risk from CO_2 monitoring

Tracking CO_2 levels could in principle be used also for an indirect determination of the potential viral charge in ambient n(t) from equation (5) and hence for real time estimations of the risk function R(t) [34]. Measuring carbon dioxide in schools is not a novelty [35–37] but linking the measured concentrations to infection risk levels is matter of ongoing research [34,38,39]. At the basis of this rationale we make here two observations: 1. time evolution of n(t) and $C_{CO2}(t)$ as air components follows similar exponential laws and 2. the instantaneous emission rates ERq(t) and ER_{CO2} (t) also follow similar time-evolutions in a homogeneous group where all persons show the same average habits. Eventually, ERq(t) and ER_{CO2}/S_0 (t) are in principle generated by the same infective subject at the same time point t. And, if the source is not known, all the subjects are equally probable infective sources in a probabilistic sense. Furthermore, if one compares equations (5) and (8), it is clear that CO_2 and n(t) saturate and decay in similar fashion, so they are certainly related, except for the k and λ factors (since viral quanta may inactivate whereas carbon dioxide does not). These factors, however, seem negligible compared to the much higher AER factors as due to ventilation, which act on both n(t) and $C_{CO2}(t)$ with the same values in equations (5) and (8). For the above-mentioned reasons, one could try to simplify their relation when considering the average effect of CO_2 and quanta emission over time, introducing a fixed direct proportion (which obviously introduces an important approximation):

$$\overline{ER}_{q_{viral}} \approx \alpha \overline{ER}_{CO_2} \Big/ S_0 \tag{16}$$

Equation (16) should be interpreted as follows: considering time-averages, the emission of viral quanta by an infective source can be related to the average CO_2 emission rate over the "emission time" by the same subject, which is $\overline{ER}_{CO_2}/S_0$. In (10) the α parameter [quanta/liter$_{CO2}$] can be determined from a known situation where the viral and the CO_2 emission rates are known. For a single "breathing resting person" reported SARS-CoV2 values are in the range of ER_q = 10–15 quanta/h/person [19] whereas $\overline{ER}_{CO_2}$ = 0.0044 l/s/person (for healthy young ages <20 years old [40]) so that α ≅0.79±0.16 quanta/liter$_{CO2}$.

Once $\overline{ER}_{CO_2}$ has been derived from the CO_2 saturation ramp of the first lesson, the viral charge n(t) could then be estimated from equation (3) and the risk function $R(t) = 1 - e^{-p\int_0^T n(t)dt}$ could be obtained as:

$$R(t>t_1) \sim 1 - e^{-p\int_0^T \left\{ \frac{\alpha\overline{ER}_{CO_2}/S_0}{IVRR} + \left[n_0 - \frac{\alpha\overline{ER}_{CO_2}/S_0}{IVRR} \right] e^{-IVRRt} \right\} dt} \tag{17}$$

by inputting an approximated but "measured" $\overline{ER_q}$from (16). It is noted that $\overline{ER}_{CO_2}$ is the result of what really happened after the first lesson in terms of group-average breathing/speaking activity and room ventilation in that particular classroom.

The whole procedure is illustrated in Fig. 3 with a real-time example measurement of CO_2 concentration taken in a real classroom. The parameter $\overline{ER}_{CO_2}$ was back-fitted from the increase of CO_2 over time from t = 0 when all scholars entered classroom and lesson started. This estimation follows a previous AER fitting using equation (9) and monitoring the CO_2 decay after all scholars exited classroom. In order to provide instantaneous risk predictions for the residual exposure time after the first hour, one could think to use AER values from literature for the first day and "learned" values for the next days, or alternatively deriving AER from the first CO_2 ramp at the first hour (this approach however, introduces additional uncertainty because the CO_2 ramp is used to derive two unknown parameters, whereas monitoring the decay after school-end has the advantage of no emission source and therefore no assumption on $\overline{ER}_{CO_2}$ which is well known only for fixed activities like "normal breathing"). The main message of Fig. 3 is: an istant CO_2 value (measured data in black) does not directly correpond to an infection risk level, nor the CO_2 signal alone is enough for proper infection risk assessment (for instant by setting thresholds on the CO_2 levels). One has to derive the whole Risk Function (red curve in Fig. 3b) after calculating n(t) for the remaining exposure time and verify that such function always satisfies the zero-infection condition (eq. 11). This can be done by monitoring also the number of susceptibles over time (S) and the airing factors (AER) over time to be used in eq. 17 (where IVRR ≈ AER + λ).

3. Results and discussion

Calculated airborne risk curves in a classroom of 170 m^3 with one infective source based on the thermally extended GN-Riley model are plotted in Fig. 4a–d while time evolution of the total viral charge in ambient is shown in Fig. 5. The infective teacher case is shown in Fig. 4a and b, while Fig. 4c and d shows the infective student case for comparison. Different risk levels after 5h are summarized in Table 2 for a fixed intermediate mask effectiveness of 75% whereas Fig. 4 shows the complete range of mask effectivness.

3.1. Natural ventilation during the cold- and hot season

In this study we explored the influence of 4 different airing cycles of the AER function (two for winter and two for summer conditions). Long and short winter cycles corresponding to 10/50 and 20/100 "break over lesson time ratio" (duration in minutes) were supposed for each simulated scenario, giving rise to dashed and solid risk curve in Fig. 4. In summer, a constant AER value has been supposed due to the possibility to keep windows open throughout the school day. Remarkably, the deviation of the first curves (in red) from reference ("no mitigations") highlights the significant impact of natural ventilation alone on risk mitigation (face masks were intentionally not included in the first scenarios to isolate the net contribution of air ventilation to the decrease of the infection risk). This reduction reads about 70–80% (in log scale) at lectures' end. The additional mitigation effect of surgical masks (under the assumption they are worn by all subjects) causes a further risk mitigation of 35–45% from the previous vales (depending on the effective time they are properly worn). In winter, shorter (but more frequent) breaks perform better than longer ones in all risk curves (dashed lines lower than solid lines). Manual airing combined with

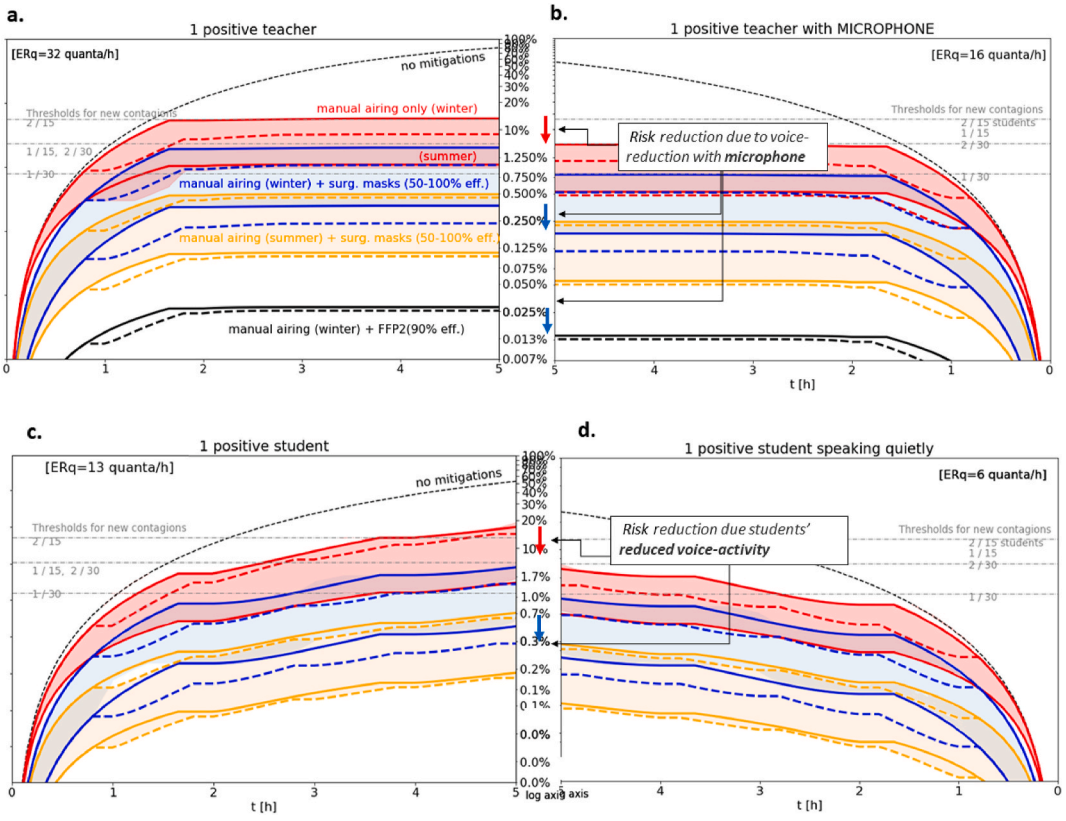

Fig. 4. Mitigation of airborne risk in a classroom (V_{eff} = 150 m^3) through face masks and ventilation. a) Infective teacher standing and teaching. b) Infective teacher speaking more quietly with mask + microphone + amplifier (−40% ER_q). c) Normal infective student case. d) Infective student speaking at moderate voice volume. Partial ventilation (AER = 2 vol/h) was assumed during breaks (continuous plots refer to long ventilation cycles, dashed plots to short cycles). Please note FFP2 masks were only considered for teacher according to recent Italian school regulation [41].

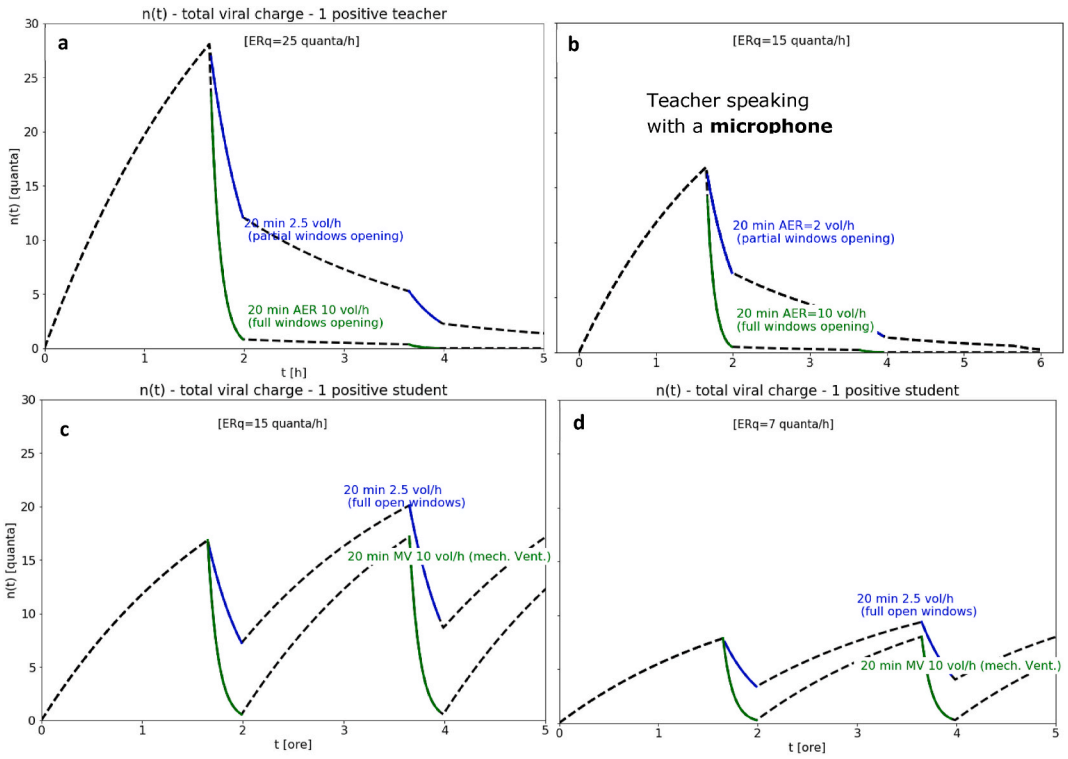

Fig. 5. Total viral load in classroom. a) teacher speaking for 2h at normal voice volume. b) teacher speaking more quietly through a microphone + voice amplifier. Partial and full windows opening scenarios in winter are also compared.

Table 2
Summary of airborne infection risk values at the end of a school day in different conditions. All individuals are wearing surgical masks and classroom volume V is fixed to 150 m^3.

Source	Ventilation during breaks [Vol/h]	Source emission timespan [h]	Face-mask effectiveness	$\overline{ERq_j}$ range[quanta h-1]	$\overline{\overline{ERq}}$ [quanta h-1]	R_c (5h)
Teacher	2	2h	75%	1–80	32	6.6%
	10	2h	75%			3.3%
Teacher with microphone	2	2h	75%	0.5–30	16	3.3%
	10	2h	75%			1.6%
Student	2	5h	75%	0.7–60	13	5.6%
	10	5h	75%			3.25%
Student speaking quietly	2	5h	75%	0.2–20	6	3.1%
	10	5h	75%			1.8%

protective mask perform better during the hot-season (yellow region) vs cold-season (blue region): in spite of lower AER values, summer airing cycles can be much more prolonged (windows in summer can in principle stay open the entire school day).

3.2. *Infective teacher vs infective student*

Teacher risk curves increase more steeply in the first 2 h of exposure time when compared to infective student curves (Fig. 4a vs 4c). This is due to the higher average emission rate of a teaching person compared to a student sitting on a desk and speaking less frequently. In case a teacher is equipped with a microphone connected to a voice amplifier, a reduced emission rate by almost 40% lowers down the risk levels for the exposed group considerably. This decrease in the final infection risk value is about −20% if considering natural ventilation as the only mitigation combined with teacher's microphone, and up to −40% when further adding the surgical masks (red and blue arrows in the middle of Fig. 4a and b). In case of a positive student source, one can still differentiate between students speaking normally and students speaking at a moderate volume (Fig. 4d). Although a microphone passed from student to student must be excluded as possible direct infection source, a more feasible scenario could be that of scholars expressly required to speak quietly. In this case, the cumulative risk levels would decrease even more: a relative delta of −50% can be observed for all curves after 5 h exposure time. This fact can be explained with a more prolonged exposure of individuals to the infective source (5h instead of 2h) and, at the same time, a larger timespan for the mitigation effect to act (voice reduction). After the teacher has left the room, the ER_q in that room drops to zero, but the viral charge previously emitted by him/her will still be present for the next hours until the end of the lesson (although it will lower down after several ventilation cycles — as indicated from n(t) plots in Fig. 5). According to the GN risk model, thus, rest viral load is responsible for a further (although lower) increase of R_c during the next hours, even if the teacher source is no longer present.

The case of an infective student shows some important differences in the shape and final level of risk curves. Higher levels are caused by the risk still increasing after half exposure time whereas teacher curves saturate earlier to lower levels (Fig. 4c and d). This fact is eventually due to the infective student source re-entering classroom after each break and emitting until the end of the lessons. On the other hand, the one-

infection thresholds are reached earlier in case of an infective teacher (blue and black curves intersecting the dotted gray lines in Fig. 4a–c). This fact would confirm that crowded classes with 30 or more students are a more dangerous situation in case of an infective teacher source.

3.3. Reducing the voice level of infective sources

In case of overcrowded classes equipping the teacher with a microphone plus amplifier system would be a valuable mitigation countermeasure. Moreover, due to the lowering of one-contagion-threshold, crowded classes of 30 students in limited volumes ($V < 170\ m^3$) should be avoided. A recommended alternative would be the splitting of the class in smaller groups alternating in face-to-face mode (Fig. 6). As a rule, keep the number of students per classroom as low as possible helps reducing the contagion risk because obviously the infection threshold lowers as N increases.

3.4. Classroom volume

As illustrated in Figs. 6 and 7, the second most relevant factor after natural ventilation affecting the airborne risk is the *classroom volume* (which could actually be the first factor if one compares different classroom sizes with identical airing policy and identical Aw/V ratio). In classrooms of doubled volume (300 m^3 instead of 150 m^3 – see Fig. 7) with the same AER(t) function, the infection probability after 5h according to the GN-model is almost the half with both source cases (infective teacher or infective student). Remarkably, this reflects a common situation in *historical buildings*, where the room height may increase considerably from standard 3 m height (Fig. 7a vs Fig. 7b).

3.5. Class-splitting and voice reduction

In authors' view, the most important recommendation which should be considered in a risk mitigation strategy in schools is the splitting of large classes with unfavorable (i.e. too high) N/V ratio. The analysis of the risk graphs of previous Fig. 4a and c suggest a critical value of N/V at around 0.15. When an infective source has entered classroom (I = 1), the one-infection-threshold by aerosolization as plotted in Fig. 4a–c (dashed gray lines) is reached much earlier from the risk function R(t) in case of N=S=30 instead of N=S=15 susceptibles (intersections with the blue risk curves). This means that situations with 30 or more students in limited volumes causing an N/V ratio >0.15 should be avoided. To prevent this scenario, splitting the class group in two smaller groups, by alternating face-to-face and remote mode at every other day, would be recommended (Fig. 8). Moreover, considering a single school day, the probability of finding one (or more) infective students in a classroom at lesson's start reduces by half with the half number of students per day. As a more general rule, keeping the number of students per classroom N as low as possible helps reducing both direct and indirect possible infections at the end of the day. The reason is intuitive (although it cannot be accounted by the GN-Riley model): the aerosol cloud is expanding from source during the transient before diluting over the entire volume (and satisfying the perfect mixing hypothesis). During this expansion, it may reach earlier a higher number of people enclosed in the same

Fig. 6. High-school classrooms of different types by height and volume located in Verona (Northern Italy):
a. historical building b. standard school building.

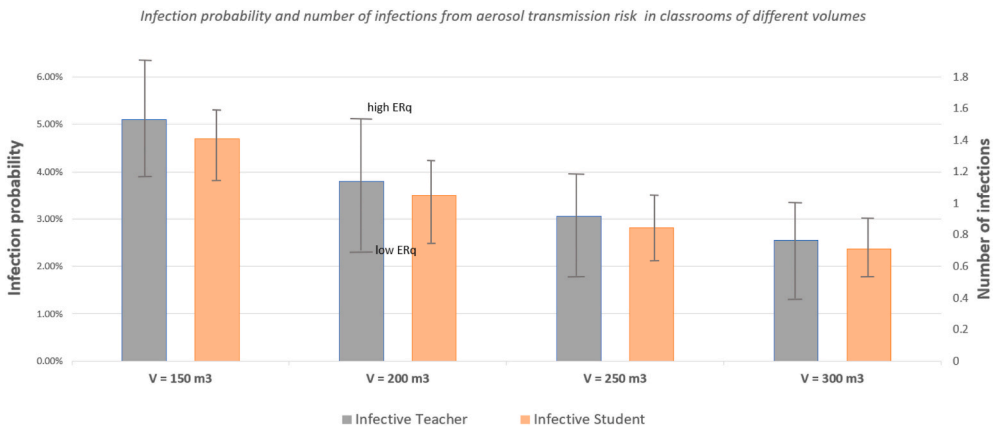

Fig. 7. Effect of the classroom volume on the infection probability R_{5h} calculated with the GN model with the same parameters except volume (75% face mask effectiveness, surgical masks, IVRR = 5.5 vol/h at each interval). Please note the infection risk (R_{5h}) is mathematically independent of the starting number of susceptible (S_0), which only influences the number of new infections at the end of the day C= S_0 *R_{5h}.

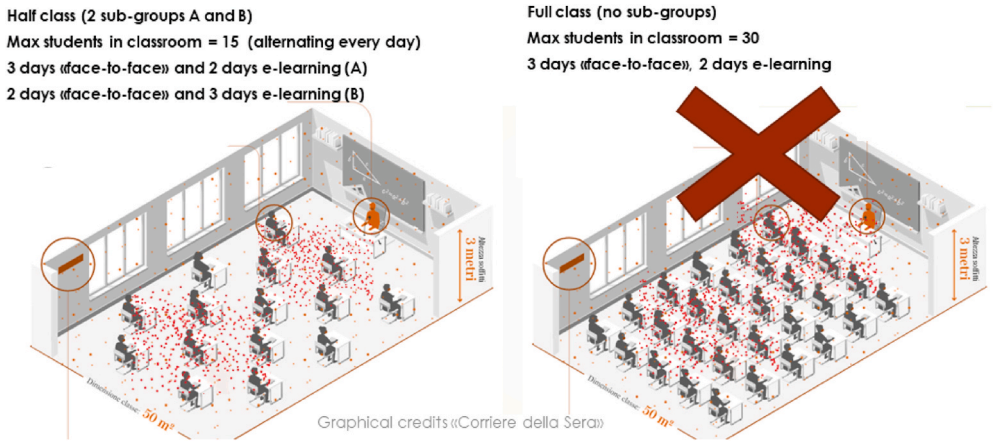

Fig. 8. Half classes in face-to-face mode (with rotating subgroups) vs full classes on alternate days. In the latter (unrecommended) case one may note the increased number of students in contact with the viral cloud emitted by the infective source.

volume in case of a higher N/V ratio (see Fig. 8 for a visual example). Secondly, the number of possible close-contact interactions would also decrease for lower N/V values.

In case a high occupancy/volume ratio cannot be avoided, equipping the teacher with a microphone plus amplifier would be a valuable countermeasure to contain aerosolization risk and still try to meet the safety requirements in terms of reproduction number ($R_0^{airborne} < 1$). This is due to a decrease in the emission rate from the potential viral source with the higher average emission rate (the teacher in a school or the lecturer in a university hall or the speaker in an auditorium). This reduction is readily visible comparing the final risk values in Fig. 4a with those of Fig. 4c (speaker with microphone and lower ERq). In the latter case and considering the worse scenario of 30 students (N/V = 0.17), the one-infection-threshold is practically never overcome by the risk function, also considering all possible effective wearing-time of protective masks (as different for the case without microphone).

4. Conclusions

Cumulative airborne risk is the key to understand indirect infections of SARS-CoV-2 in classrooms and possible outbreaks within a school building. The mitigation of the airborne risk in schools is linked to the main and larger goal of keeping most schools open and safe during the present and possible future pandemics, while pursuing at the same time a zero-infection strategy. Although the dynamic single-zone model employed here contains some important approximations and some uncertainties in the parameter estimations, the general framework is robust as it was already tested for influenza and tuberculosis. Adapted to the Covid-19 case, the GN-Riley model provided clear indications for contagion risk minimization. Firstly, students and teachers are exposed in schools for relatively long time to viral aerosol and to rely only on sanitation/ventilation cycles cannot lower the residual viral load nor the risk to zero. On the other hand, airborne risk values can be mitigated to reasonable levels by a combination of several other mitigation factors. In the present situation where most schools are still not equipped with dedicated HVAC systems, nor dedicated sensors for controlling air ventilation and filtering at the classroom level, the regular opening of classroom windows at well-defined intervals can be an effective (although provisional) solution. Regular windows opening acts indeed as mitigation co-factor which alone almost halves the airborne risk. On the other hand, the numerical analysis confirms that only a combination of air exchange with protective masks properly worn by all exposed subjects can reduce the airborne transmission risk to acceptable safe levels. Splitting crowded classes of 30 students into smaller alternating groups of 15 has also a dramatic beneficial effect on the collective contagion risk. This is ultimately due to the volumetric nature of the aerosol cloud (Fig. 8). Concerning more specific countermeasures, it has been shown that equipping teachers with microphone and voice amplifier as well as requesting students to speak quietly during lessons are effective and feasible mitigation factors to keep the airborne risk

levels below safety thresholds.

CO_2 sensors combined with infection risk models could also play an important role in risk assessment providing precise real time adjustment of the airing times. Under certain hypothesis, the information provided by the sensor could be used to feed predictive infection risk models like the GN-Riley shown here or more sophisticated ones [27], with empirical *in-situ* data and hence provide real-time feedback to control the SARS-CoV2 aerosolization risk in classrooms (as illustrated in Section 2.9, also verifying that the condition on the reproduction number – $R_0^{airborne} < 1$ - is satisfied during the whole exposure time – see Fig. 3c). In the theoretical scheme proposed by Stabile et al. [34] a CO_2 sensor could feed a central unit with experimental AER measurement from the CO_2 decay. The central unit, further instructed with external inputs like classroom volume, ERq values of SARS-CoV2 and the number of presents at a given time, could then calculate the risk function and dynamically control it by adjusting the airing schedule for that specific classroom. Such a feedback-based system could in principle be an interesting alternative to fixed a-priori scheduling of windows opening, since it could predict the time evolution of the risk function after the first airing cycle and alert the people for the next cycles when it is the right moment to manual air the room and for how long (adjusting both values, if required, to assure the zero-contagion condition is satisfied until lessons' end). However, as stressed by the same authors and as confirmed by our in-situ live measurement illustrated in Fig. 3, some uncertainty factors may affect this methodology, which, on the other hand is intrinsically more powerful and accurate than direct thresholding on absolute CO_2 levels. The risk model approach feeded by CO_2 monitoring requires to fit precise and affordable values for all the airing factors active in a real school situation (as discussed in section 2.3). This approach would also require some investment costs at the national scale [42] because all school classrooms should be provided with at least one CO_2 sensor and a process unit. Investigating this promising approach, however, is of primary interest and further research as well as on-field practices are encouraged. Parallelly, investigating an optimum risk control strategy based on pre-determined fixed manual airing cycles, remains of interest to cover also those many schools worldwide lacking advanced sensor technology and HVAC systems.

In this study we shown through mathematical models, how the desired goal of keeping the indirect infection risk from aerosolization safety below the one-infection-threshold during each school day, could in principle be achievable in any situation, provided a suitable combination of mitigation factors is implemented. However, it is also remarked that the illustrated strategy based on natural ventilation was suggested as a compromise emergency solution. For the middle and long-term future, equipping schools with dedicated HVAC systems driven by CO_2 sensors and advanced risk models remains the n.1 to-be-preferred option concerning not only infection risk mitigation but also, in a wider sense, indoor air quality, energy efficiency and thermal comfort.

Concerning safety regulations, the high sensitivity of the infection risk to classroom volume and the 3D nature of aerosol diffusion suggest a revision of social distancing norms in schools. There is a clear need for a new volumetric approach to ensure a minimum "volume per capita" for viral charge dilution (and lowering of infection risk). While linear social distancing (varying from 1 m to 2 m in different EU countries) could be maintained, new safety criteria based on the occupancy/volume ratio should be considered. For instance, higher minimum required classroom heights (and therefore larger minimum classroom volumes) based on target occupancy should be considered for new constructions and for major retrofitting works. Some historical buildings, indeed, already had larger classroom spaces compared to recent buildings due to higher internal walls (up to 50–80% higher than in standard modern school buildings, as clearly visible in Fig. 7). Classrooms compliant for linear social distancing but small in height, should be furtherly checked to guarantee a minimum height (and volume) in order to sufficiently dilute a viral aerosol cloud even in case of insufficient ventilation levels (typical of the winter season). To this regard, schools in historical buildings, while usually lacking the possibility to install HVAC systems, could more easily be compliant with the volumetric classroom requirement and hence be maintained as school seats with minor interventions like the installation of air quality sensors in each classroom. Schools not provided with HVAC systems but with critically small classrooms (where the zero-infection-threshold could not be guaranteed event with frequent airing cycles) could adopt for those classrooms one of the illustrated additional mitigations: student group splitting alternating face-to-face lessons and/or amplified audio systems for teachers.

We conclude with a statistical remark. As previously noted, in regions where the likelihood of one or more asymptomatic source seems particularly high or to increase steeply, a class splitting strategy would be highly recommended, particularly for large groups ($\geq$25 students). However, to be more precise we should base this decision on the probability to have one or more asymptomatic sources in a classroom (the present study already assumes one asymptomatic source in a classroom). Therefore, there is a need to solve an open statistical problem: the estimation of the local probability function $p_{local}\,(I \geq 1 \mid N_{age})$ of having at least one asymptomatic source (but they could be even more than one) in a classroom, i.e. in random ensemble of N students of given age located in a certain region, given the local epidemic situation in that particular area, city or district.

Authorship

All listed authors meet the ICMJE criteria.
We attest that all authors contributed significantly to the creation of this manuscript, each having fulfilled criteria as established by the ICMJE.

We confirm that the manuscript has been read and approved by all named authors.

We confirm that the order of authors listed in the manuscript has been approved by all named authors.

Authorship contribution statement

A.Zivelonghi: Conceptualization, Methodology, Measurements, Writing original draft. M. Lai: Post-Processing support, Draft Correction, Discussions.

Funding

No funding was received for this work.

Declaration of competing interest

The authors declare that they have no known competing financial interests or personal relationships that could have appeared to influence the work reported in this paper.

Acknowledgements

The authors want to thank G. Buonanno, L.Morawska, E.Zio and L. Moccia for insightful discussions.

Appendix A. Supplementary data

Supplementary data to this article can be found online at https://doi.org/10.1016/j.buildenv.2021.108139.

APPENDIX

A.1 Cumulative risk

Applying a Wells-Riley like approach to model a situation where susceptibles are cyclic leaving the environment during breaks, requires to clarify the concept of cumulative risk. It is firstly noted that no new source beside the initial one should be considered during the exposure time, even in case a new infection occurred in that time, since any new infected person needs an incubation time of some days before becoming infective.

Let us consider now the total number of infections occurred in a classroom (after a certain number of classes and breaks): the variable of practical interest is not the single risk function during a single lecture, $R_{lec,i}(t)$, (which starts from zero after each break), but rather the *cumulative risk* $R_{c,i}(t)$ at the time t, which keeps into account the whole "history" of infection risk up to that time-point:

$$R_{cum,i}(t) = \frac{C_i\left(t - (i-1)\left(t^{lec}+t^{brk}\right)\right) + \sum_{j=1}^{i-1} C_j\left(t_j^{lec}, n_{0j}\right)}{S_0} = R_i\left(t - (i-1)\left(t^{lec}+t^{brk}\right)\right) + \sum_{j=1}^{i-1} R_j\left(t_j^{lec}, n_{0j}\right) \tag{A.1}$$

In (10), $C_j(t)$ represents the number of infections in the previous hours and the index j spans all the "cycles" of lecture + break before the current i-lesson (j = 1 to i-1, assuming cyclic lecture + breaks of duration $t_{lec} + t_{brk}$). $R_i(t)$ is the infection probability during the i-cycle which is actually a dual function:

$$R_i(t) = \begin{cases} R_{lec,i}(t_i) = 1 - e^{\left[-\frac{p}{V}\overline{ER_q}\phi_i\left(t_i,\ n_{0,i},\ \overline{ER_q},\ AER\right)\right]} & if\ \ 0 \le t_i \le t^{lec} \\ R_{brk,i}(t_i) = 0 \quad if\ \ t^{lec} < t_i < t^{lec} + t^{brk} \end{cases} \tag{A.2}$$

The same for the viral load in ambient:

$$n_i(t) = \begin{cases} n_{lec,i}(t_i) = \dfrac{\overline{ER_q}}{IVRR} + \left[n_0 - \dfrac{\overline{ER_q}}{IVRR}\right] e^{-IVRR \cdot t_i} & if\ \ 0 \le t_i \le t^{lec} \\ n_{brk,i}(t_i) = \left[n_{lec,i}\left(t_i^{lec}\right)\right] e^{-IVRR\left(t+t_i^{lec}\right)} & if\ \ t^{lec} < t_i < t^{lec} + t^{brk} \end{cases} \tag{A.3}$$

Two python routines which implement equations (A.1-A.3) recursively were separately developed for the infective teacher as well as for the infective student case.

When the infective source is removed from the environment, the ERq parameter in equations (A.2) and (A.3) turns zero. However, the overall infection risk $R_{cum}(t)$ remains greater than zero. This because it must keep memory of previous contagions (as a probability measure linked to the total emitted viral charge). Mathematically, this is assured by the historical sum in (A.1) and by the multiplicative exponential factor $\phi_i(t,\ n_{0,i},\ 0,\ AER)$ non-zero even if one source left room ($ER_q = 0$) because of the residual cumulated viral load previously emitted in the same room ($n_{lec,i}(t_i) \neq 0$) and because the residual viral charge cannot suddenly drop to zero (finitness of the airing factor AER).

Table A1
Estimations of $\overline{\overline{ERq}}$ values adopted in simulations

	Voice Activity	$ER_{q,min}$	$ER_{q,max}$	$\overline{ERq_j}$	t_{br}	$t_{sp,low}$	t_{sp_normal}	$\overline{\overline{ERq}}$	±σ
		(quanta/h)			(% time)			(quanta/h)	
Teacher	normal	1	80	40,5	15	10	75	32,1	±6,2
	low	0,5	30	15,25					
	breathing	0,1	2	1,05					
Teacher + microphone	normal	1	80	40,5	15	75	10	15,4	±3,0
	low	0,5	30	15,25					
	breathing	0,1	2	1,05					
Student	normal	0,7	70	35,35	65	0	35	13,1	±2,5
	low	0,2	20	10,1					
	breathing	0,1	2	1,05					
Student speaking quietly	normal	0,7	70	35,35	65	35	0	6,0	±1,2
	low	0,2	30	15,1					
	breathing	0,1	2	1,05					

References

[1] L. Morawska, D. K Milton, It is Time to Address Airborne Transmission of COVID-19, Clinical Infectious Diseases, ciaa939, https://doi.org/10.1093/cid/ciaa939.

[2] H. Qian, T. Miao, L. Liu, X. Zheng, D. Luo, Y. Li, "Indoor transmission of SARS-CoV-2", Indoor Air (2020) 1–7, https://doi.org/10.1111/ina.12766, 00.

[3] Felicity Aiano, et al., COVID-19 outbreaks following full reopening of primary and secondary schools in england: retrospective, cross-sectional national surveillance, January 14, Available atSSRN, https://ssrn.com/abstract=3766014, 2021, http://doi.org/10.2139/ssrn.3766014.

[4] Italian Health Institut (ISS) - Report ISS COVID-19 n. 63/2020 "Apertura delle scuole e andamento dei casi confermati di SARS-CoV-2: la situazione in Italia" pp. 16..

[5] Otte im Kampe, Eveline, et al., Euro Surveill. 25 (2020) 2001645, https://doi.org/10.2807/1560-7917.ES.2020.25.38.2001645. Surveillance of COVID-19 school outbreaks, Germany, March to August 2020.

[6] "Covid nella Marca, le classi focolaio sono 164". ("Covid in the Marca Region, school outbreaks are 164") Tribuna Treviso local newspaper. https://tribunatreviso.gelocal.it/treviso/cronaca/2021/04/26/news/covid-nella-marca-le-classi-focolaio-sono-164-a-scuola-il-virus-dilaga-1.40201563.
[7] C. Stein-Zamir, N. Abramson, H. Shoob, et al., A large COVID-19 outbreak in a high school 10 days after schools' reopening, Israel, May 2020, Euro Surveill. 25 (29) (2020) 2001352, https://doi.org/10.2807/1560-7917.ES.2020.25.29.2001352.
[8] D. Tosi, A.S. Campi, How schools affected the COVID-19 pandemic in Italy: data analysis for lombardy region, campania region, and emilia region, Future Internet 13 (2021) 109, https://doi.org/10.3390/fi13050109.
[9] L. Morawska, Julian W. Tang, W. Bahnfleth, et al., How can airborne transmission of COVID-19 indoors be minimised? Environ. Int. 142 (2020) 105832, https://doi.org/10.1016/j.envint.2020.105832. ISSN 0160-4120.
[10] Y. Li, G.M. Leung, J.W. Tang, X. Yang, C.Y. Chao, et al., Role of ventilation in airborne transmission of infective agents in the built environment—a multidisciplinary systematic review, Indoor Air 17 (2007) 2–18.
[11] N.H.L. Leung, D.K.W. Chu, E.Y.C. Shiu, et al., Respiratory virus shedding in exhaled breath and efficacy of face masks, Nat. Med. 26 (2020) 676–680, https://doi.org/10.1038/s41591-020-0843-2.
[12] A.R. Escombe, C.C. Oeser, R.H. Gilman, et al., Natural ventilation for the prevention of airborne contagion, PLoS Med. 4 (2) (2007) e68. https://doi:10.1371/journal.pmed.0040068.
[13] C.Zunino reporting on ARPA Piemonte study in cooperation with antiviral research laboratory "San Luigi Gonzaga", Orbassano– "Virus in quali luoghi ce n'è di più. Inesistente all' aperto, concentrazioni alte nelle case". https://www.repubblica.it/scienze/2021/01/12/news/ora_si_potra_avvistare_il_covid_nell_aria-282183617/.
[14] A. Zivelonghi, The airborne risk transmission of SARS-CoV-2 in high- schools estimated with a single zone dynamic model", AiCARR Journal 64 (5) (2020) 49–54.
[15] E.C. Riley, G. Murphy, R.L. Riley, Airborne spread of measles in a suburban elementary school, Am. J. Epidemiol. 107 (5) (1978 May) 421–432, https://doi.org/10.1093/oxfordjournals.aje.a112560. PMID: 665658.
[16] L. Gammaitoni, M.C. Nucci, Using a mathematical model to evaluate the efficacy of TB control measures, Emerg. Infect. Dis. 3 (1997) 335–342.
[17] David Marr, Mark Mason, Ron Mosley, Xiaoyu Liu, The Influence of Opening Windows and Doors on the Natural Ventilation Rate of a Residential Building, The Free Library, 2012 (January, 1), https://www.thefreelibrary.com/The influence of opening windows and doors on the natural ventilation...-a0282940533.
[18] S.E. Chatoutsidou, M. Lazaridis, Assessment of the impact of particulate dry deposition on soiling of indoor cultural heritage objects found in churches and museums/libraries, J. Cult. Herit. 39 (2019) 221–228, https://doi.org/10.1016/j.culher.2019.02.017.
[19] G. Buonanno, L. Stabile, L. Morawska, Estimation of airborne viral emission: quanta emission rate of SARS-CoV-2 for infection risk assessment, Environ. Int. 141 (2020) 105794, https://doi.org/10.1016/j.envint.2020.105794. ISSN 0160-4120.
[20] EN16798-7 "Energy Performance of Buildings - Ventilation for Buildings Part 7: Calculation Methods for the Determination of Air Flow Rates in Buildings Including Infiltration (Modules M5-5), "6.4.3.5.4 – Calculation of Ventilation through Windows Using Wind Velocity and Temperature Difference as Input".
[21] N. van Doremalen, T. Bushmaker, D.H. Morris, M.G. Holbrook, A. Gamble, B. N. Williamson, A. Tamin, J.L. Harcourt, N.J. Thornburg, S.I. Gerber, J. O. LloydSmith, E. de Wit, V.J. Munster, Aerosol and surface stability of SARS-CoV-2 as compared with SARS-CoV-1, N. Engl. J. Med. (2020), https://doi.org/10.1056/NEJMc2004973.
[22] M. Abuhegazy1 e, et al., Num. investigation of aerosol transport in a classroom with relevance to COVID-19, Phys. Fluids 32 (2020) 103311, https://doi.org/10.1063/5.0029118.
[23] J. Allen, J. Spengler, E. Jones, J. Cedeno-Laurent, 5-step guide to checking ventilation rates in classrooms. Technical report, Harvard. https://schools.forhealth.org/wp-content/uploads/sites/19/2021/01/Harvard-Healthy-Buildings-program-How-to-assess-classroom-ventilation-10-30-2020-EN_R1.8.pdf, 2020.
[24] J. Smereka, K. Ruetzler, L. Szarpak, K.J. Filipiak, M. Jaguszewski, Role of Mask/respirator Protection against SARS-CoV-2. Anesthesia and Analgesia, 10.1213/ANE.0000000000004873, Advance online publication, 2020, https://doi.org/10.1213/ANE.0000000000004873.
[25] Amy V. Mueller, Matthew J. Eden, Jessica J. Oakes, Chiara Bellini, Loretta A. Fernandez, Quantitative method for comparative assessment of particle filtration efficiency of fabric masks as alternatives to standard surgical masks for PPE edRxiv, 04.17.20069567, https://doi.org/10.1101/2020.04.17.20069567, 2020.
[26] D.K. Milton, A rosetta stone for understanding infectious drops and aerosols, Sep 17, J Pediatric Infect Dis Soc 9 (4) (2020) 413–415, https://doi.org/10.1093/jpids/piaa079. PMID: 32706376; PMCID: PMC7495905.
[27] K. Mahjoub Mohammed Merghani, B. Sagot, E. Gehin, G. Da, C. Motzkus, A review on the applied techniques of exhaled airflow and droplets characterization, Indoor Air 31 (2021) 7–25, https://doi.org/10.1111/ina.12770.
[28] G. Zayas, M.C. Chiang, E. Wong, et al., Cough aerosol in healthy participants: fundamental knowledge to optimize droplet-spread infectious respiratory disease management, BMC Pulm. Med. 12 (2012) 11, https://doi.org/10.1186/1471-2466-12-11.
[29] L. Morawska, G.R. Johnson, Z.D. Ristovski, M. Hargreaves, K. Mengersen, S. Corbett, C.Y.H. Chao, Y. Li, D. Katoshevski, Size distribution and sites of origin ofdroplets expelled from the human respiratory tract during expiratory activities, J. Aerosol Sci. 40 (2009) 256–269, https://doi.org/10.1016/j.jaerosci.2008.11.002.
[30] Y. Pan, D. Zhang, P. Yang, L.L.M. Poon, Q. Wang, Viral load of SARS-CoV-2 in clinical samples, Lancet Infect. Dis. 20 (4) (2020), https://doi.org/10.1016/S1473-3099(20)30113-4.
[31] K.K.-W. To, O.T.-Y. Tsang, W.-S. Leung, A.R. Tam, T.-C. Wu, D.C. Lung, C.C.-Y. Yip, J.-P. Cai, J.M.-C. Chan, T.S.-H. Chik, D.P.-L. Lau, C.Y.-C. Choi, L.-L. Chen, W.-M. Chan, K.-H. Chan, J.D. Ip, A.C.-K. Ng, R.W.-S. Poon, C.-T. Luo, V.C.-C. Cheng, J. F.-W. Chan, I.F.-N. Hung, Z. Chen, H. Chen, K.-Y. Yuen, Temporal profiles of viral load in posterior oropharyngeal saliva samples and serum antibody responses during infection by SARS-CoV-2: an observational cohort study, Lancet Infect. Dis. (2020), https://doi.org/10.1016/S1473-3099(20)30196-1.
[32] G. Buonanno, L. Stabile, L. Morawska, Quantitative assessment of the risk of airborne transmission of SARS-CoV-2 infection: prospective and retrospective applications, Environ. Int. 145 (December) (2020), https://doi.org/10.1016/j.envint.2020.106112, 106112 ISSN 0160-4120.
[33] S. Asadi, A.S. Wexler, C.D. Cappa, et al., Aerosol emission and superemission during human speech increase with voice loudness, Sci. Rep. 9 (2019) 2348, https://doi.org/10.1038/s41598-019-38808-z.
[34] L. Stabile, A. Pacitto, A. Mikszewski, L. Morawska, G. Buonanno, Ventilation procedures to minimize the airborne transmission of viruses in classrooms, Build. Environ. 202 (2021) 108042, https://doi.org/10.1016/j.buildenv.2021.108042. ISSN 0360-1323.
[35] J.M. Daisey, W.J. Angell, M.G. Apte, Indoor air quality, ventilation and health symptoms in schools: an analysis of existing information, Indoor Air 13 (2003).
[36] Z. Bakò-Biro, D.J. Clements-Croome, N. Kochhar, H.B. Awbi, M.J. Williams, Ventilation rates in schools and pupils' performance, Build. Environ. 48 (2012) 215–223.
[37] L Stabile, M Dell'Isola, A Russi, A Massimo, G Buonanno, The effect of natural ventilation strategy on indoor air quality in schools, Sci. Total Environ. 1595 (2017 Oct) 894–902, https://doi.org/10.1016/j.scitotenv.2017.03.048.
[38] A. Di Gilio, J. Palmisani, M. Pulimeno, F. Cerino, M. Cacace, A. Miani, G. de Gennaro, CO_2 concentration monitoring inside educational buildings as a strategic tool to reduce the risk of Sars-CoV-2 airborne transmission, Environ. Res. 2202 (2021 Jul) 111560, https://doi.org/10.1016/j.envres.2021.111560.
[39] Z Peng, J.L. Jimenez, Exhaled CO_2 as a COVID-19 infection risk proxy for different indoor environments and activities, Environ. Sci. Technol. Lett. 8 (5) (2021) 392–397, https://doi.org/10.1021/acs.estlett.1c00183.
[40] A. Persily, L. de Jonge, Carbon dioxide generation rates for building occupants, Indoor Air 27 729 (2017) 868–879, https://doi.org/10.1111/ina.12383.
[41] Italian Ministry of Education, note n. 698 of 6th of May 2021, concerning "Profilassi vaccinale in favore del personale scolastico, docente e non docente. Mascherine FFP2. Piani di sicurezza – Aggiornamenti in tema di emergenza Covid-19".
[42] L. Moccia - Technical report, Rischio COVID-19 via Aerosol nelle Scuole Note bibliografiche, esempi di interventi, e loro dimensionamento. https://www.researchgate.net/publication/351441612_Rischio_COVID-19_via_Aerosol_nelle_Scuole_Note_bibliografiche_esempi_di_interventi_e_loro_dimensionamento, 2021.